

Island-size distributions in submonolayer epitaxial growth: Influence of the mobility of small clusters

M. C. Bartelt

Institute for Physical Research and Technology, Iowa State University, Ames, Iowa 50011

S. Günther, E. Kopatzki, and R. J. Behm

Abteilung Oberflächenchemie und Katalyse, Universität Ulm, D-89069 Ulm, Germany

J. W. Evans

Department of Mathematics and Ames Laboratory, Iowa State University, Ames, Iowa 50011

(Received 14 July 1995; revised manuscript received 31 October 1995)

We examine the influence of dimer mobility on the size distribution of two-dimensional islands formed by irreversible nucleation and growth during deposition. We first characterize the transition in scaling of the mean island density with increasing dimer mobility, from the classic form described by Venables [Philos. Mag. **27**, 697 (1973)] to the modified form for “rapid” mobility described by Villain *et al.* [J. Phys. (France) I **2**, 2107 (1992)]. The corresponding transition in the asymptotic scaling function describing the shape of the island-size distribution is then also characterized. In addition, we contrast the mean-field form of the scaling function for rapid dimer mobility with that for zero mobility. Analysis of experimental data for Au/Au(100), Fe/Fe(100), Cu/Cu(100), and Pt/Pt(111) homoepitaxy reveals no clear evidence for a regime of modified island density scaling due to rapid dimer mobility. However, for Fe/Fe(100) below 400 K, we argue that mobility of small clusters significantly influences the shape of the island-size distribution, even before it affects the mean island density.

I. INTRODUCTION

For submonolayer nucleation and growth of islands during deposition, the behavior of the mean island density N_{av} and of the full island size distribution are of primary interest. Typically, analyses of these quantities allow for a general critical size i , above which islands (or clusters) are stable against dissociation, but ignore the mobility of stable islands.¹⁻³ For isotropic (two-dimensional) surface diffusion, a classic mean-field rate-equation analysis¹⁻³ then predicts that N_{av} scales with deposition flux F and substrate temperature T as

$$N_{\text{av}} \sim (F/\nu)^\chi \exp[\chi\beta(E_d + i^{-1}E_i)] \\ \sim (h_1/F)^{-\chi} \exp[\beta E_i/(i+2)], \quad (1)$$

where $\chi = i/(i+2)$, for fixed coverage θ and large h_1/F . Here, we have set $\beta = 1/(k_B T)$, $h_1 = \nu \exp(-\beta E_{d1})$ denotes the hop rate for isolated adatoms (determined by the diffusion barrier E_{d1} and attempt frequency ν), and $E_i \geq 0$ denotes the binding energy for the critical cluster with i atoms (so $E_1 = 0$). In general, one expects a transition from a regime of irreversible island formation where $i=1$, at low T , to some type of $i>1$ behavior for higher T where adatom-adatom bond scission becomes operative. Details depend on the model or system, and on the specific values of key parameters.³⁻⁷

A possible complication of the above scenario for $i=1$ can arise if dimers or other stable clusters become “sufficiently mobile” before single-bond scission becomes operative. Then Villain *et al.*⁸ have shown via a mean-field analysis that the scaling behavior of N_{av} is modified from the

above $i=1$ form. This was recently confirmed by simulations.⁹ Specifically, if monomers hop at rate h_1 (as above), and dimers hop at rate $h_2 = \nu \exp(-\beta E_{d2})$, but trimers and larger clusters are immobile, then one has^{8,9}

$$N_{\text{av}} \sim (F/\nu)^{2/5} \exp[\beta(E_{d1} + E_{d2})/5] \sim (h_1 h_2 / F^2)^{-1/5}, \quad (2)$$

for fixed θ and sufficiently large h_2 (relative to h_1) and h_1/F . A mean-field derivation of (2) is also provided below.

Next we comment on what behavior is possible or likely to occur in physical systems. It is known that dimer diffusion can sometimes occur relatively easily via a “twisting motion” (through diagonal nearest-neighbor configurations) or “exchange” on metal (100) surfaces, and via a “concerted motion” on metal (111) surfaces.¹⁰ In either case, the motion has a much lower activation barrier than dimer dissociation.¹⁰ Thus one expects dimer hop rates to often dominate dissociation rates. Based on this observation, Liu, Bönig, and Metiu⁹ argued that, typically, mobility of small clusters will significantly affect the island density before the transition to $i>1$ behavior occurs. They appropriately emphasize that the possibility of modified scaling (2) should be routinely considered in the analysis of experimental data. However, we note that the work of Villain *et al.*⁸ also shows that dimer hop rates dominating dissociation rates is *not* sufficient to guarantee a regime of modified scaling (2), before the onset of $i>1$ behavior (see below). Thus it is possible to make a direct transition from classic $i=1$ behavior (1) to $i>1$ behavior,¹¹ without an intermediate regime of modified scaling (2). Indeed, none of the specific systems we examine here show clear evidence of a regime of modified scaling (2).

Assuming that only monomers and dimers are mobile, Villain *et al.*⁸ elucidate scaling behavior in nucleation and growth by a simple comparison of the following key rates:¹² $H_{\text{agg}} \sim h_1 N_1$, the aggregation rate at which each dimer is “hit” and immobilized by diffusing monomers of density N_1 ; $H_{\text{loss}} \sim h_2 N_{\text{av}}$, the rate at which each dimer is “lost” due to diffusion-mediated aggregation with stable islands; and $H_{\text{diss}} \sim h_1 \exp(-\beta E_{\text{bond}})$, the dissociation rate for each dimer with bond strength E_{bond} . There are three distinct regimes.⁸

(i) $H_{\text{agg}} \gg H_{\text{loss}}$ and H_{diss} . Dimers are quickly immobilized, and larger, more stable islands are formed, before dimer mobility or dissociation become effective. Classic $i=1$ scaling (1) results.

(ii) $H_{\text{loss}} \gg H_{\text{agg}}$ and H_{diss} . Loss of dimers as potentially stable islands, due to their diffusion and aggregation with other stable islands, significantly reduces N_{av} relative to case (i), while dimer dissociation is still ineffective. Modified scaling (2) results.

(iii) $H_{\text{diss}} \gg H_{\text{agg}}$ and H_{loss} . Dimer dissociation is more important than dimer mobility, and $i>1$ behavior results.

Thus modified scaling (2) requires not just that $h_2 \gg H_{\text{diss}}$, but that $H_{\text{loss}} \gg H_{\text{diss}}$, or equivalently that $h_2 \gg H_{\text{diss}}/N_{\text{av}}$ (where typically $N_{\text{av}} \ll 1$). Clearly, cluster dissociation has an intrinsically greater effect on N_{av} than does cluster mobility.

In this paper, we analyze the effect of dimer mobility on the island-size distribution for irreversible nucleation and growth of islands during deposition. We first characterize the transition in the scaling of the mean island density N_{av} from the classic $i=1$ form (1) to the modified form (2), with the increase of a natural crossover parameter related to the ratio $\mathcal{R} = H_{\text{loss}}/H_{\text{agg}}$. We also characterize the corresponding transition in the shape of the asymptotic scaling function for the island-size distribution from its well-known form when $\mathcal{R} = h_2 = 0$. In particular, we show that, even when dimer mobility does not affect the classic $i=1$ value (or scaling) of N_{av} , it can have a significant effect on the island-size distribution. We then focus on the regime of significant dimer mobility ($\mathcal{R} \gg 1$), and present an analytic form for the associated mean-field scaling function. Finally, we present some applications to specific homoepitaxial metal systems, including Au/Au(100), Fe/Fe(100), Cu/Cu(100), and Pt/Pt(111), none of which appear to display modified scaling (2).

II. $i=1$ POINT-ISLAND MODEL WITH DIMER MOBILITY

In this study, we consider only the regime of low coverage below about $\theta=0.1$ – 0.15 ML, where the influence of the finite extent of islands (and, in particular, island coalescence and next-layer nucleation) is insignificant. We thus use a “point-island” model where islands or clusters occupy single sites, but carry a label to indicate their size.¹³ Such models have been shown to accurately reproduce size distributions for more realistic models with compact islands, in this low- θ regime.¹⁴ Specifically, in our model, monomers are deposited randomly on a square lattice of adsorption sites at rate F per site, isolated monomers hop at rate h_1 and dimers hop at rate h_2 between adjacent sites, and larger clusters are immobile. (Modification to include mobility of larger clusters is straightforward.) Island nucleation and growth are irreversible. Thus, whenever two diffusing monomers meet, they ir-

reversibly nucleate an island. Whenever a monomer diffuses to or is deposited adjacent to a (point) island, or whenever a dimer diffuses to a (point) island, it is irreversibly incorporated into that island. These events result in an increase in the island-size label. Of primary interest is the evolution in time (t) of the distribution of densities, N_s , of islands of size s . Here N_1 gives the density of monomers (as above), N_2 gives the density of dimers, etc.; $N_{\text{av}} = \sum_{s>2} N_s$ and $\theta = Ft = \sum_{s \geq 1} s N_s$.

A. The simulation algorithm

The behavior of the above model can be determined effectively exactly via Monte Carlo simulation. At each simulation time step, either an atom is deposited at a randomly chosen site, or a randomly chosen monomer is moved, or a randomly chosen dimer is moved. These different types of events are selected with probabilities $F/(F+h_1 N_1+h_2 N_2)$, $h_1 N_1/(F+h_1 N_1+h_2 N_2)$, and $h_2 N_2/(F+h_1 N_1+h_2 N_2)$, respectively. Irreversible aggregation is implemented whenever monomers or dimers are adjacent to islands (or to each other), and then island-size labels are appropriately incremented. We use a 512×512 square lattice with periodic boundary conditions, and average measured quantities over $O(10^3)$ runs.

B. Mean-field analysis

Mean-field rate equations for the island-size distribution N_s in this model are obtained by considering all processes leading to the gain or loss of islands of a certain size due to deposition, or due to diffusion-mediated aggregation of monomers and dimers with islands.^{1–3} The aggregation rate for monomers ($j=1$) or dimers ($j=2$) with islands of size s is taken as $K h_j N_j N_s$, where $K=O(1)$ denotes a size-independent “capture number” (cf. Ref. 1), appropriate to the point-island model. If we retain only dominant terms for $H_{\text{loss}} \gg H_{\text{agg}}$, and invoke a steady-state approximation for both N_1 and N_2 , then the rate equations adopt the simplified form

$$\begin{aligned} dN_1/dt &\approx F - K h_1 N_1 N_{\text{av}} - K(h_1 + h_2) N_1 N_2 - 4K h_1 N_1^2 \\ &\approx F - K h_1 N_1 N_{\text{av}} \approx 0, \end{aligned} \quad (3a)$$

$$\begin{aligned} dN_2/dt &\approx 2K h_1 N_1^2 - K(h_1 + h_2) N_1 N_2 - K h_2 N_2 N_{\text{av}} \\ &\quad - 4K h_2 N_2^2 \\ &\approx 2K h_1 N_1^2 - K h_2 N_2 N_{\text{av}} \approx 0, \end{aligned} \quad (3b)$$

$$\begin{aligned} dN_{s>2}/dt &\approx K h_1 N_1 (N_{s-1} - N_s) + K h_2 N_2 (N_{s-2} - N_s) \\ &\approx K h_1 N_1 (N_{s-1} - N_s). \end{aligned} \quad (3c)$$

The scaling behavior (2) for $N_{\text{av}} = \sum_{s>2} N_s$, in the regime of $H_{\text{loss}} \gg H_{\text{agg}}$, is recovered by first summing (3c) over all $s>2$ to obtain

$$\begin{aligned} dN_{\text{av}}/dt &\approx K(h_1 + h_2) N_1 N_2 \\ &\approx K h_1 N_1 N_2 \quad (\text{if } h_1 \text{ dominates } h_2). \end{aligned} \quad (4)$$

One then uses the steady-state relations $N_1 \approx F/(Kh_1N_{av})$ and $N_2 \approx h_1N_1^2/(h_2N_{av})$ to obtain a closed equation for N_{av} , integration of which recovers (2).

III. RESULTS

A. Crossover scaling

From the discussion in Sec. I, one expects that the key parameter characterizing the transition from the classic $i=1$ scaling (1) to the modified scaling (2) is given by the ratio $\mathcal{R} = H_{\text{loss}}/H_{\text{agg}}$. We show that this is the case by first analyzing the transition, with increasing \mathcal{R} , in the exponent χ which characterizes the scaling of $N_{av} \sim F^\chi$ with F , as $F \rightarrow 0$. χ should vary from the classic value of $\frac{1}{3}$, for $\mathcal{R} \ll 1$ [cf. Eq. (1) with $i=1$], to $\frac{2}{3}$, for $\mathcal{R} \gg 1$ [cf. Eq. (2)]. Before presenting the results of this analysis, it is instructive to examine in more detail the natural crossover parameter,

$$\mathcal{R} = H_{\text{loss}}/H_{\text{agg}} \approx (h_2/h_1)(N_{av}/N_1) \approx (h_2/F)(N_{av})^2, \quad (5)$$

where we have used the steady-state relation $F \approx h_1N_1N_{av}$ (see Sec. II C). One can show that \mathcal{R} always depends on the same combination

$$Z = (h_2/F)^3(h_1/F)^{-2} = (\nu/F)\exp[-\beta(3E_{d2} - 2E_{d1})] \quad (6)$$

in *both* the high- and low-dimer-mobility regimes, despite the fact that N_{av} scales *very differently* in these two regimes. Specifically, one finds that

$$\mathcal{R} \sim Z^{1/3} \quad \text{for } \mathcal{R} \ll 1 \quad \text{and} \quad \mathcal{R} \sim Z^{1/5} \quad \text{for } \mathcal{R} \gg 1. \quad (7)$$

Note also that invariably $3E_{d2} - 2E_{d1} > 0$, so \mathcal{R} increases with increasing T , which would lead to a transition from the classic $i=1$ scaling (1) to the modified scaling (2). We remark, as an aside, that a crossover parameter (analogous to \mathcal{R}) characterizing transitions in critical size i with increasing T has been identified.⁷ In addition, a reduction of this parameter to a simpler, more explicit form (analogous to Z) has been noted and utilized.⁷

In Fig. 1, we show simulation and rate-equation results for the “universal curve” of χ versus Z . Similar behavior follows from plotting χ versus \mathcal{R} ; however the variable Z may often be more useful in practice. For example, from the crossover curve, we can identify $Z \approx 10^{-3}$ as the value where classic $i=1$ scaling starts to break down. Then, given the knowledge of the activation energies, one can use the explicit formula for Z to determine the associated transition temperature. Alternatively, given E_{d1} and an experimental value for the transition temperature, one can determine E_{d2} from the condition that $Z \approx 10^{-3}$. We should remark on the evident deviations from classic values of exponents in the limiting regimes of \mathcal{R} , and on deviations from “universality” in Fig. 1. Both derive from values of h_1/F (and h_2/F) which are not “asymptotically large.” Furthermore, incorporating appropriate logarithmic corrections^{8,13} to the classic rate-equation theory significantly slows the convergence to asymptotic exponent values, as noted by Liu, Böning, and Metiu.⁹ Finally, we have also confirmed the prediction of (2) for the Arrhenius behavior of N_{av} , when $h_1 \approx h_2$, as was done in Ref. 9.

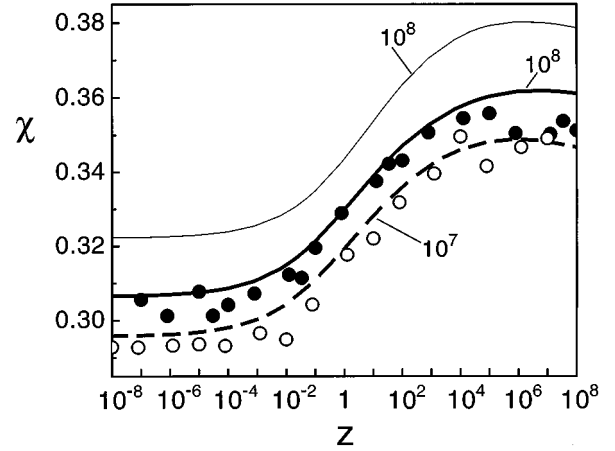


FIG. 1. Transition in the effective flux-scaling exponent χ from simulations with increasing $Z = (h_2/F)^3(h_1/F)^{-2}$. We used $h_1/R = 10^7$ (\circ) and 10^8 (\bullet). The *thick solid lines* give results from rate equations including logarithmic corrections (Ref. 13), with $h_1/R = 10^7$ (dashed) and 10^8 (solid). The *thin solid line* is from rate equations without logarithmic corrections, and $h_1/R = 10^8$. The coverage is 0.1 ML.

B. Island-size distributions

Next we turn to the focus of this paper, namely, characterizing the island-size distribution N_s . For a range of low (precoalescence) coverages θ and in the regime of *large* mean island size, $s_{av} \approx \theta/N_{av}$, this distribution should satisfy^{3-5,13,14}

$$N_s \sim \theta(s_{av})^{-2} f(s/s_{av}). \quad (8)$$

Here $f()$ is a scaling function which describes the shape of the distribution, and satisfies $\int_0^\infty f(x) dx = \int_0^\infty x f(x) dx = 1$ since $N_{av} = \sum_{s>2} N_s$ and $\theta = \sum_{s \geq 1} s N_s$. While (8) applies for all $s \geq 1$ when $h_2 = 0$ (cf. Ref. 13), it should only apply for $s > 2$ when, e.g., $h_2 \approx h_1$ (see below).

One obviously expects different forms for the scaling function f for zero dimer mobility and for “rapid” dimer mobility. Furthermore, based on the above crossover analysis, one also expects that the scaling function f is naturally parametrized by the crossover variable Z (or \mathcal{R}). Figure 2 shows the evolution of the “asymptotic” scaling function with increasing Z . Specifically, we show f for $Z=0$ (no dimer mobility), 10^2 (the crossover region), and 10^8 (rapid dimer mobility), where $f(0) \approx 0.37$, 0.30 , and 0.23 , respectively. Here we have set $h_1/F = 10^8$, and varied $h_2/h_1 = 0$, 0.01 , and 1 (with fixed $\theta = 0.1$ ML), for which $\mathcal{R} = H_{\text{loss}}/H_{\text{agg}} = 0$, ~ 1 , and ~ 31 , respectively. An entirely analogous parametrization of the scaling function for the island-size distribution was described in the simulation studies of Ratsch *et al.*,⁶ where the focus was on the onset of bond scission, rather than on dimer mobility.

Another general issue is that of convergence to the asymptotic scaling form of the island-size distribution with increasing s_{av} or h_1/F (for fixed Z). This has been examined in detail for $i=1$ and no dimer mobility^{13,14} ($Z=0$). Figure 3 shows this convergence in the regime of “rapid” dimer mobility or large Z , specifically for $h_2 = h_1$ and increasing h_1/F .

Finally, we have also analyzed the full infinite coupled set of linear equations (3a)–(3c) for N_s , for large Z or \mathcal{R} , to

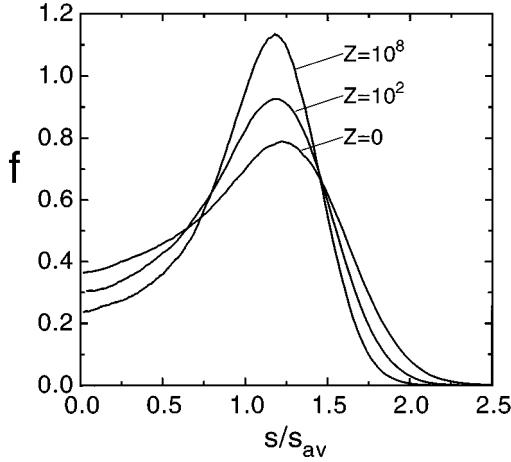


FIG. 2. Simulation results for the transition in the scaling function $f=[(s_{av}^2)/\theta]N_{s>2}$ with increasing $Z=0, 10^2$, and 10^8 , corresponding to $h_1/F=10^8$ and $h_2/h_1=0, 0.01$, and 1 , respectively. Here $\theta=0.1$ ML, $\mathcal{R}=H_{\text{loss}}/H_{\text{agg}}=0, \sim 1$, and ~ 31 , and $s_{av}\approx 62, 73$, and 139 atoms, respectively.

determine the corresponding mean-field form of the scaling function f . This involves combining generating function techniques, with a steepest-descent analysis for the asymptotic regime of large h_1/F or s_{av} . (See Ref. 13 for details of a corresponding analysis in the case where $h_2=0$.) In this way, we obtain for $Z\gg 1$ the mean-field prediction

$$f_{\text{MF}}(0\leq x < \frac{5}{4}) \approx \frac{1}{5} [1 - \frac{4}{5}x]^{-3/4} \quad \text{and} \quad f_{\text{MF}}(x > \frac{5}{4}) = 0. \quad (9)$$

One should compare (9) with the prediction^{3,13} for $Z\ll 1$ (or actually $Z=h_2=0$) of $f_{\text{MF}}(0\leq x < \frac{3}{2}) \approx \frac{1}{3} [1 - \frac{2}{3}x]^{-1/2}$ and $f_{\text{MF}}(x > \frac{3}{2}) = 0$. Thus the mean-field theory predicts a nonzero $f(0)$ which is reduced from $\frac{1}{3}$ for limited dimer mobility ($Z\ll 1$) to $\frac{1}{5}$ for “rapid” dimer mobility ($Z\gg 1$). This behavior is consistent with our simulations, but contrasts with recent suggestions⁵ that $f(0)=0$. However, as noted previously,^{3,13} we believe the feature that $f_{\text{MF}}(x)$ diverges at some $x>1$, and is strictly zero thereafter, is an artifact of the neglect of

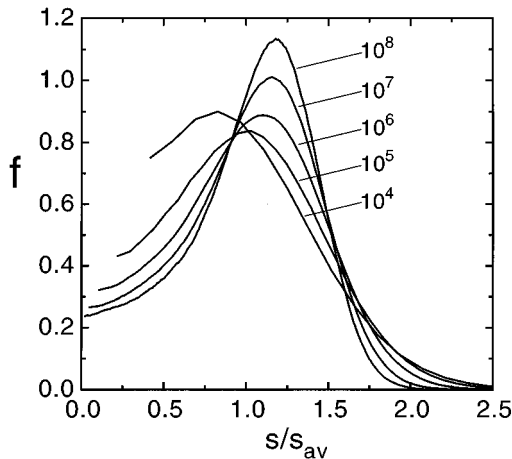


FIG. 3. Simulation results for the scaling function $f=[(s_{av}^2)/\theta]N_{s>2}$ at 0.1 ML for $h_1=h_2$ and $h_1/F=10^4-10^8$ where $\mathcal{R}=H_{\text{loss}}/H_{\text{agg}}\approx 4, 7, 12, 19$, and 31 , and $s_{av}\approx 7, 14, 28, 61$, and 139 atoms, respectively.

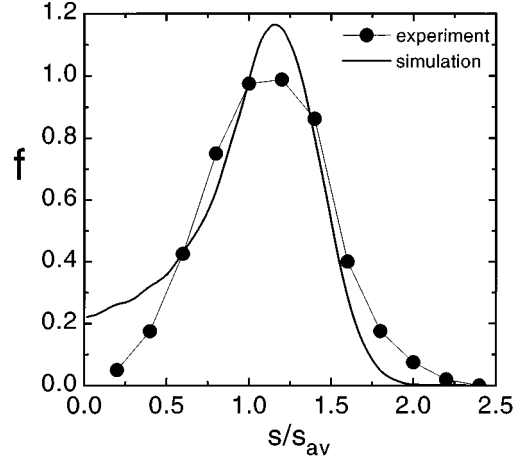


FIG. 4. Scaled island-size distribution for Au on “hex”-reconstructed Au(100) at 315 K. Symbols are experimental data for $\theta\approx 0.08$ ML and $F\approx 0.5$ ML/min. The line is the simulation result for $E_{d1}=E_{d2}=0.4$ eV and $\nu=10^{13}$ /s, which match the experimental Arrhenius slope and value of $N_{av}\approx 3.7\times 10^{-4}$ /site. Here $\mathcal{R}=H_{\text{loss}}/H_{\text{agg}}\approx 45$.

certain fluctuations in the mean-field approximation. This issue will be discussed in detail elsewhere.¹⁵

IV. ANALYSIS OF SPECIFIC SYSTEMS

We now apply the above results to the analysis of some specific homoepitaxial metal systems.

Au on “hex”-reconstructed Au(100)

Studies of nucleation and growth during deposition for this system¹⁶ showed that $N_{av}\sim F^{0.37\pm 0.03}$ at 315 K, and also revealed an Arrhenius slope for N_{av} of ~ 0.17 eV in the range $T=315-380$ K. The observed χ is marginally consistent with classic results for $i=1$ with isotropic diffusion and no dimer mobility, but our simulations^{13,14} yield a value for N_{av} which is 7–10 times higher than the experimentally observed value of $\sim 3.7\times 10^{-4}$ /site for $F=0.5$ ML/min. Instead, for reasons discussed further below, it was proposed¹⁶ that diffusion on the “hex”-reconstructed Au(100) surface is strongly anisotropic. Then the above data were fitted with $i=3$, $E_{d1}\approx 0.2$ eV, and $E_{\text{bond}}\approx E_3/2\approx 0.3$ eV. A somewhat poorer fit of the Arrhenius slope with $i=2$, $E_{d1}\approx 0.2$ eV, and $E_{\text{bond}}=E_2\approx 0.23$ eV should not be discounted,¹⁶ particularly since $i=2$ (stable trimers) might be expected given the locally (111) structure of the “hex”-reconstructed surface. Either choice also consistently fits the behavior for $T>400$ K, where the Arrhenius slope of N_{av} is larger, corresponding to a larger i .

In contrast, Liu, Bönig, and Metiu⁹ argue that strongly anisotropic diffusion is unlikely in this system. By assuming isotropic diffusion and *significant* dimer mobility, they fitted the data with $i=1$, $E_{d1}\approx E_{d2}\approx 0.4$ eV (or $E_{d1}\approx 0.35$ eV and $E_{d2}\approx 0.45$ eV), and $\nu=10^{13}$ /s. Our “point-island” simulations with these parameters confirm their fit of the N_{av} behavior, and produce the island-size distribution shown in Fig. 4 for 0.08 ML (where the “point-island” model is applicable). However, this distribution appears to differ significantly from the experimental distribution, also shown, bringing into question this interpretation of Liu, Bönig, and

Metiu.⁹ One cannot unequivocally rule out their interpretation because of statistical uncertainty in the experimental data. Also, the presence of any coarsening (not included in our modeling) would modify the predicted size distribution, specifically reducing the densities of smaller islands to match experiment more closely.

Liu, Bönig, and Metiu⁹ motivate their reanalysis of the Au/Au(100) data by arguing that the (111)-like structure of the “hex” reconstruction is inconsistent with strong anisotropy. However, this local picture of the reconstruction is oversimplistic. Scanning tunneling microscope (STM) images of the clean Au(100) surface¹⁶ show a dramatic “striped structure,” which persists throughout the nucleation process. Diffusion need not be truly one dimensional, but just restricted primarily along individual strips (5 lattice spacings wide) in order for the original analysis to apply, as noted in Ref. 15. The broad 200-Å-wide zones denuded of islands at steps orthogonal to these stripes and the almost complete lack of denuded zones at steps parallel to them are certainly consistent with such strongly anisotropic diffusion.¹⁷ Furthermore, a recent effective-medium theory (EMT) study of this system¹⁸ by the authors of Ref. 9 indeed finds anisotropic diffusion along the above-mentioned strips. The EMT value for the lowest activation barrier for monomer diffusion is also much closer to the estimate of Ref. 16 than to that of Ref. 9.

Finally, we briefly remark on yet another possible interpretation of the original data for this system.¹⁶ Here we assume isotropic diffusion, as in Ref. 9, and neglect dimer mobility for simplicity, but allow for bond scission rather than prescribing $i=1$. Then choosing $E_d \approx 0.32$ eV and $E_{\text{bond}} \approx 0.42$ eV, we obtain $\chi = 0.37$ at 315 K, so the system has begun to make a transition^{4,6,7} to $i > 1$ behavior, reducing N_{av} to the experimental value, and still matching the Arrhenius slope of ~ 0.17 eV. However, this model does not appear to fit the observed island-size distribution at 315 K (cf. Ref. 7) nor to fit the observed N_{av} at substantially higher temperatures.

Fe on Fe(100)

STM measurements¹⁹ on this system for the full island-size distributions at $\theta = 0.07$ ML for $T < 450$ K certainly suggest that $i=1$ in this regime.³ The measured island density N_{av} is also reproduced from simulations¹⁴ with $i=1$ and no dimer mobility, choosing $E_{d1} \approx 0.45$ eV (and $\nu \approx 10^{12}$ /s) consistent with the experimental Arrhenius slope for N_{av} of ~ 0.15 eV. However, careful comparison (see Fig. 5) reveals that the experimental (expt) densities for small islands are lower than values from our realistic $i=1$ square-island simulations¹⁴ (sim) (or corresponding “point-island” simulations¹³) without dimer mobility. Specifically, one finds that $f_{\text{expt}}(0) \approx 0.2$ and $f_{\text{sim}}(0) \approx 0.4$. In contrast, simulations for $i=1$ without dimer mobility by two other groups^{5,6} appear to fit the experimental data very well, and recover $f(0) \approx 0.2$. However, we believe⁷ that these “good” fits are an artifact of the fractal island geometry incorporated into these simulations, which is not appropriate for Fe/Fe(100). We have suggested⁷ instead that the precise description of the observed size distributions must incorporate some mobility of small clusters into the $i=1$ model. Results of such a modification to an $i=1$ “point-island” model are shown in Fig. 5

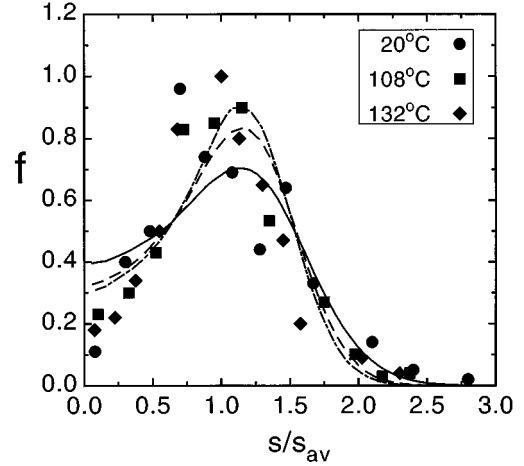


FIG. 5. Scaled island-size distribution for Fe/Fe(100). Symbols are experimental data (Ref. 19) for $\theta \approx 0.07$ ML, $F \approx 0.7$ ML/min, and the temperatures indicated. Lines are simulation results at 20 °C with $E_{d1} = 0.45$ eV and $\nu = 4 \times 10^{12}$ /s. Solid: no cluster mobility. Dashed: dimer mobility with $E_{d2} = 0.55$ eV and $H_{\text{loss}}/H_{\text{agg}} \approx 1$. Dot-dashed: dimer and trimer mobility with $E_{d2} = E_{d3} = 0.55$ eV and $H_{\text{loss}}/H_{\text{agg}} \approx 1$. All choices match the experimental Arrhenius slope and value of $N_{\text{av}} \approx 3 \times 10^{-3}$ /site.

for 0.07 ML (where the “point-island” model is applicable). However, it is also possible that some coarsening has occurred before STM imaging, reducing the density of smaller islands, and producing the observed lower $f(0)$.

We emphasize that our modeling of this system, including a “small” amount of dimer (and trimer) mobility, does *not* significantly modify the value of N_{av} or its scaling with F from the classic $i=1$ form (1). However, one might ask if it is possible to reinterpret clean Arrhenius behavior for Fe/Fe(100) in the whole regime of $T < 450$ K in terms of modified scaling due to rapid dimer mobility. We show that this is *not* the case. Using (2), one requires $(E_{d1} + E_{d2})/5 \approx 0.15$ eV, so $E_{d1} \leq 0.375$ eV assuming that $E_{d1} \leq E_{d2}$. Clearly, this produces island densities much lower than observed in the experiment since both lowering E_{d1} and inclusion of dimer mobility yield lower N_{av} . Thus we believe that this system does *not* display modified scaling (2), despite the expectations of Ref. 9.

Cu on Cu(100)

A relatively complete set of diffraction studies has been performed on this system.^{20,21} Thus it is appropriate to examine these data in detail to determine if a regime of modified scaling (2) is manifested (cf. Ref. 9). From measurement of the ring diameter d^* of the diffracted intensity profile, behavior of the real-space correlation length $l_c \sim 1/d^*$ was determined. For deposition of 0.3 ML of Cu, the Arrhenius slope of l_c displayed an apparent jump from ~ 0.06 eV for $T < 223$ K to ~ 0.12 eV for $T > 223$ K. See Ref. 20 for details.

Assuming that $l_c \sim N_{\text{av}}^{-1/2}$, the behavior for $T < 223$ K (where $i=1$) might correspond to either (A) $E_{d1} \approx 0.36$ eV for limited dimer mobility;²⁰ or (B) significant dimer mobility with, e.g., $E_{d1} \approx E_{d2} \approx 0.3$ eV. An independent measurement²¹ of $\chi \approx \frac{1}{3}$ at 223 K suggests (A). Also, using square-island simulations,¹⁴ we matched the observed value

of d^* assuming (A) in Ref. 7, but would certainly obtain a much smaller d^* assuming (B). If the break in slope for $T > 223$ K was due to the onset of significant dimer mobility (still with $i=1$), then one must have $E_{d1} + E_{d2} \approx 1.2$ eV, so $E_{d2} \approx 0.8$ eV which is much too high for dimer mobility to be significant. Instead, this break was interpreted in Ref. 20 as a sharp transition to classic $i=3$ scaling, producing an anomalously low estimate of $E_{\text{bond}} \approx 0.06$ eV (e.g., inconsistent with $i=1$ below 223 K). In fact, we find that the observed behavior does not correspond to a true break in the Arrhenius slope, but rather to a gradual transition out of the $i=1$ regime due to the onset of dimer dissociation with $E_{\text{bond}} \approx 0.2$ eV. See Ref. 7 for a detailed discussion.

Pt on Pt(111)

The mean island density measured in STM studies²² at 205 K was shown in Ref. 23 to correspond to an activation barrier for monomer diffusion of 0.25 eV (choosing $\nu = 10^{12}$ /s), if one assumes irreversible island formation ($i=1$) with negligible cluster mobility. In fact, this value was later confirmed by direct field-ion microscopy observations.²⁴ Finally, a more recent comprehensive com-

parison of experimental observations of nucleation and growth with simulation finds near perfect agreement with an $i=1$ model *excluding* cluster mobility.²⁵ Thus, despite reasonable expectations,⁹ it does not appear that dimer mobility significantly affects N_{av} at (or below) 205 K.

V. SUMMARY

For irreversible nucleation and growth of two-dimensional islands during deposition, we have provided a comprehensive characterization of the influence of dimer mobility on the island-size distribution. We have demonstrated how this characterization is important for analysis of behavior in specific homoepitaxial metal systems, even though we find no examples of systems displaying the modified scaling of Villain *et al.*,⁸ due to “rapid” dimer mobility.

ACKNOWLEDGMENTS

The work of M.C.B. and J.W.E. was supported by NSF Grant No. CHE-9317660. It was performed at Ames Laboratory which is operated for the U.S. DOE by Iowa State University under Contract No. W-7405-Eng-82.

-
- ¹J. A. Venables, G. D. T. Spiller, and M. Hanbücken, Rep. Prog. Phys. **47**, 399 (1984).
- ²S. Stoyanov and D. Kaschiev, in *Current Topics in Materials Science Vol. 7*, edited by E. Kaldis (North-Holland, Amsterdam, 1981), pp. 69–141.
- ³J. W. Evans and M. C. Bartelt, J. Vac. Sci. Technol. A **12**, 1800 (1994); for two-dimensional (2D) diffusion and general critical size i , the mean-field scaling function for the island-size distribution was determined here to be $f_{\text{MF}}(x) = (i+2)^{-1} [1 - (i+1)(i+2)^{-1}x]^{-i/(i+1)}$.
- ⁴C. Ratsch, A. Zangwill, P. Šmilauer, and D. D. Vvedensky, Phys. Rev. Lett. **72**, 3194 (1994).
- ⁵J. G. Amar and F. Family, Phys. Rev. Lett. **74**, 2066 (1995).
- ⁶C. Ratsch, P. Šmilauer, A. Zangwill, and D. D. Vvedensky, Surf. Sci. **328**, L599 (1995).
- ⁷M. C. Bartelt, L. S. Perkins, and J. W. Evans, Surf. Sci. Lett. **344**, L1193 (1995); M. C. Bartelt and J. W. Evans (unpublished).
- ⁸J. Villain, A. Pimpinelli, L. Tang, and D. Wolf, J. Phys. (France) I **2**, 2107 (1992); J. Villain, A. Pimpinelli, and D. Wolf, Comments Condens. Matter Phys. **16**, 1 (1992).
- ⁹S. Liu, L. Bönig, and H. Metiu, Phys. Rev. B **52**, 2907 (1995).
- ¹⁰G. L. Kellogg, Surf. Sci. Rep. **21**, 1 (1994); S. Liu, Z. Zhang, J. Nørskov, and H. Metiu, Surf. Sci. **321**, 161 (1994); C.-L. Liu, *ibid.* **316**, 294 (1994); S. C. Wang and G. Ehrlich, *ibid.* **239**, 301 (1990); A. F. Voter, Proc. SPIE **821**, 214 (1988).
- ¹¹Note that classic treatments of the $i > 1$ regime *implicitly* incorporate mobility of dimers and other substable clusters in a quasi-equilibrium Walton relation (Refs. 1–3).
- ¹²We ignore the minor contribution to immobilization and loss of dimers due to dimer-dimer collisions.
- ¹³M. C. Bartelt and J. W. Evans, Phys. Rev. B **46**, 12 675 (1992); M. C. Bartelt, M. C. Tringides, and J. W. Evans, *ibid.* **47**, 13 891 (1993).
- ¹⁴M. C. Bartelt and J. W. Evans, Surf. Sci. **298**, 421 (1993); in *Common Themes and Mechanisms of Epitaxial Growth*, edited by P. Fuoss *et al.*, MRS Symposia Proceedings Vol. 312 (Materials Research Society, Pittsburgh, 1993), p. 255.
- ¹⁵M. C. Bartelt and J. W. Evans, Bull. Am. Phys. Soc. (to be published).
- ¹⁶S. Günther, E. Kopatzki, M. C. Bartelt, J. W. Evans, and R. J. Behm, Phys. Rev. Lett. **73**, 553 (1994).
- ¹⁷As noted in Ref. 16, this effect could be due to anisotropic sticking at different steps, rather than due to anisotropic diffusion.
- ¹⁸L. Bönig, S. Liu, and H. Metiu (unpublished).
- ¹⁹J. A. Stroschio and D. T. Pierce, Phys. Rev. B **49**, 8522 (1994); J. Vac. Sci. Technol. B **12**, 1783 (1994).
- ²⁰H. Dürr, J. F. Wendelken, and J.-K. Zuo, Surf. Sci. **328**, L527 (1995).
- ²¹J.-K. Zuo, J. F. Wendelken, H. Dürr, and C.-L. Liu, Phys. Rev. Lett. **72**, 3064 (1994).
- ²²M. Bott, Th. Michely, and G. Comsa, Surf. Sci. **272**, 161 (1992).
- ²³M. C. Bartelt and J. W. Evans, Surf. Sci. **314**, L829 (1994).
- ²⁴P. J. Feibelman, J. S. Nelson, and G. Kellogg, Phys. Rev. B **49**, 10 548 (1994).
- ²⁵M. Bott, M. Hohage, M. Morgenstern, T. Michely, and G. Comsa (unpublished).